NASA TECHNICAL NOTE

NASA TN D-2284

NASA TN D-2284

ON THE USE OF A MAGNETOMETER TO DETERMINE THE ANGULAR MOTION OF A SPINNING BODY IN REGULAR PRECESSION

by George R. Young and Jesse D. Timmons

Langley Research Center

Langley Station, Hampton, Va.

NATIONAL AERONAUTICS AND SPACE ADMINISTRATION • WASHINGTON, D. C. • MAY 1964

ON THE USE OF A MAGNETOMETER TO DETERMINE THE ANGULAR MOTION OF A SPINNING BODY IN REGULAR PRECESSION

By George R. Young and Jesse D. Timmons

Langley Research Center
Langley Station, Hampton, Va.

NATIONAL AERONAUTICS AND SPACE ADMINISTRATION

For sale by the Office of Technical Services, Department of Commerce,
Washington, D.C. 20230 -- Price $0.50

ON THE USE OF A MAGNETOMETER TO DETERMINE THE ANGULAR MOTION OF A SPINNING BODY IN REGULAR PRECESSION

By George R. Young and Jesse D. Timmons
Langley Research Center

SUMMARY

An analysis is presented which deals with the use of an onboard magnetometer for determining the motion of spinning bodies in uniform precession.

Calculated curves for the variation of the magnetometer reading with time are shown for several different coning angles and orientations and also for different angles between the magnetometer axis and the body axes; these curves are used as illustrations of magnetometer-signal traces in the analysis and discussion. In particular, it is shown how the envelopes of these curves may be analyzed to yield the body coning angle and the angle between the earth's local magnetic field vector and the angular-momentum vector of the body.

INTRODUCTION

One of the difficult problems in space technology is that of determining the attitude of a spinning body within reasonable angular limits. For this purpose gyros, accelerometers, horizon scanners, and recently aspect magnetometers have been used. With the exception of the aspect magnetometer, data techniques for these instruments are readily available in the literature.

The aspect magnetometer is a device which, when placed in the earth's magnetic field, produces a voltage output proportional to the component of the earth's magnetic field along the magnetometer's sensitive (probe) direction. Reference 1 provides a detailed discussion of aspect magnetometers.

The present study derives an equation governing the time variation of this component for a spinning and precessing body having a magnetometer mounted at a known angle to the spin axis. This equation is used to calculate three distinct types of typical magnetometer histories which are later analyzed to obtain expressions for evaluating body coning angle and the angle between the local magnetic vector and the angular-momentum vector of the body.

(3) The body is assumed to be rigid.

(4) The spin rate p_0 is constant (i.e., there are no roll torques).

The case considered will be that of a spinning body which has been given an impulse about an axis perpendicular to the axis of spin. The resulting motion (ref. 6) is a precession or coning about the angular-momentum vector $\bar{H}$ of the body. The spin rate and precession rate are related (for small coning angles and the condition $I_X/I < 1$) by the equation (ref. 6)

$$\omega_p = p_0 \frac{I_X}{I} \tag{1}$$

The magnetic field component measured by the magnetometer probe at any time t is

$$B_p = B \cos \epsilon(t) \tag{2}$$

The probe is mounted at an angle γ to the longitudinal (spin) axis of the body. Figure 1 shows the geometrical relationships between the precession cone, the direction of the magnetic vector $\bar{B}$, and the cone swept out by the probe in a spin cycle. The angular velocity $\frac{d\psi}{dt}$ is the rate of precession of the body axis $\bar{p}$ about the angular-momentum vector $\bar{H}$, and $\frac{d\phi}{dt}$ is the rate of rotation of the probe vector $\bar{L}$, about the spin vector, $\bar{p}$ (see fig. 1). It can be shown that

$$\psi = \left(\psi_0 + \omega_p t\right) \tag{3}$$

$$\phi = \phi_0 + \left(p_0 - \omega_p\right)t \tag{4}$$

The angle $\epsilon(t)$ of equation (2), which determines the instantaneous reading of the magnetometer, depends on the time-dependent precession and nutation angles ψ and ϕ, the fixed angle γ, and the two angles ν and θ, which are essentially constant during the part of the flight being analyzed. The equation relating $\epsilon(t)$ to these five angles may be derived as follows:

Consider the arcs γ, θ, and ν on a unit sphere as in figure 1 with $\bar{H}$ along the Z-axis and the arc θ in the Y-Z plane. The x,y,z coordinates of the point k are ($\sin \nu \sin \psi$, $\sin \nu \cos \psi$, $\cos \nu$). Now rotate the arc segment $klmn$ through an angle θ about the X-axis so that the point m now lies on the Z-axis. Thus, a unit vector $\bar{k}$, lying along the line Ok has components ($\sin \nu \sin \psi$, $\sin \nu \cos \psi \cos \theta + \cos \nu \sin \theta$, $-\sin \nu \cos \psi \sin \theta + \cos \nu \cos \theta$). Similarly, a unit vector $\bar{n}$ lying along the line On has components ($\sin \gamma \sin \phi$, $-\sin \gamma \cos \phi$, $\cos \gamma$). Then $\cos \epsilon$ is given by the scalar product of these two unit vectors, or

$$\cos \epsilon(t) = \sin \nu \sin \psi \sin \gamma \sin \phi - \sin \nu \cos \psi \cos \theta \sin \gamma \cos \phi$$
$$- \cos \nu \sin \theta \sin \gamma \cos \phi - \sin \nu \cos \psi \sin \theta \cos \gamma$$
$$+ \cos \nu \cos \theta \cos \gamma \qquad (5)$$

The (a) parts of figures 2 to 6 are plots of $\cos \epsilon(t)$ or B_p/B as given in equations (2) and (5). The spin rate p_0 and precession rate ω_p were assumed to be 24 radians/sec and 4 radians/sec, respectively, and corresponded to an inertial ratio I_X/I of 1/6 as can be seen from equation (1). Equations (3) and (4) were substituted into equation (5) and equation (5) was then solved to generate time histories of B_p/B on a high-speed electronic data processing machine. The time of 3 seconds was chosen in order to include two complete precession cycles. The points on the curves were plotted by an automatic plotting machine which accounts for the data points on the calculated curves.

The schematic (part (b)) of figures 2 to 6 gives an idea of the progress of the probe in spinning and precessing in space and gives essentially the path in space traced out by the probe. These curves were plotted from the equations

$$\left.\begin{aligned} A_1 &= \nu + \theta \cos \psi + \gamma \cos(\psi + \phi) \\ A_2 &= \theta \sin \psi + \gamma \sin(\psi + \phi) \end{aligned}\right\} \qquad (6)$$

These equations were derived by assuming the line lk in figure 1 is fixed. The line lm is then rotating about the line Ol at the rate $\dot{\psi}$ and the line mn is rotating about the line Om at the rate $\dot{\phi}$. Equations (6) then represent this motion projected onto a plane perpendicular to $\bar{B}$ where A_1 is parallel to the line lk and A_2 is perpendicular to lk. Thus a plot of A_1 against A_2 gives a qualitative picture of the motion. The fact that the schematics do not represent the exact magnitude of the motion is of little consequence since they are intended only to help to gain an insight into the motion.

On a magnetometer trace (for the usual conditions of small inertia ratio and small coning angle) the short-period oscillations correspond approximately to the spin frequency p_0 while the long-period oscillations correspond to the precession frequency ω_p. The spin rate can be found from the magnetometer trace by averaging the time between successive short-term peaks. The precession rate can be found by averaging the time between the long-term peaks or from equation (1).

In order to analyze the magnetometer trace a curve is drawn which represents the envelope of the motion. There are some easily recognizable points on this envelope which correspond to the various cases when the vectors $\bar{B}$, $\bar{H}$, $\bar{p}$, and $\bar{L}$ all lie in the same plane.

On figure 2(a) the point A on the envelope corresponds to the condition in which the magnetic vector $\bar{B}$, the angular-momentum vector $\bar{H}$, the spin axis, and the probe axis lie in the same plane in such a manner that

$$\epsilon(t) = \nu + \theta + \gamma \tag{7}$$

The point A will be used as a reference point in calculating ψ and ϕ.

The point directly opposite A on the envelope corresponds to a rotation of the body through 180°. This point will be labeled C; its ordinate is equal to $\cos(\nu + \theta - \gamma)$.

At the point on the envelope one-half of a precession cycle from A, the ordinate is $\cos(\nu - \theta + \gamma)$. This point is labeled F. The point directly opposite F will again represent a 180° movement of the probe and will be labeled E. Its ordinate is $\cos(\nu - \theta - \gamma)$.

In summary (to simplify the nomenclature, A will be used to denote the ordinate of the point A, etc.):

$$A = \cos(\nu + \theta + \gamma);\ \phi = \phi_0 = 0;\ \psi = \psi_0 = 0 \tag{8}$$

$$C = \cos(\nu + \theta - \gamma);\ \phi = \pi;\quad \psi = 0 \tag{9}$$

$$F = \cos(\nu - \theta + \gamma);\ \phi = \pi;\quad \psi = \pi \tag{10}$$

$$E = \cos(\nu - \theta - \gamma);\ \phi = 0;\quad \psi = \pi \tag{11}$$

It is obvious from the envelope that ϕ and ψ do not, in general, attain these values simultaneously but there will be no error if the envelope is faired correctly. The accuracy of the fairing will be better if $p_0 \gg \omega_p$ because there will be more points per cycle to aid in the fairing process.

Since for any angle β, $\cos\beta = \cos(-\beta)$, equations (8) to (11) may be rewritten as

$$\cos^{-1}A = \nu + \theta + \gamma \tag{12}$$

$$\cos^{-1}C = |\nu + \theta - \gamma| \tag{13}$$

$$\cos^{-1}F = |\nu - \theta + \gamma| \tag{14}$$

$$\cos^{-1}E = |\nu - \theta - \gamma| \tag{15}$$

It is obvious from the form of equations (12) to (15) that ambiguities can arise in the determination of ν and θ. These ambiguities can generally be resolved if the characteristics of the trajectory are known. For this purpose, three cases are recognized. These three cases and the analysis for each follows:

Case I. $\nu > \theta + \gamma$

In this case equations (12) to (15) become

$$\cos^{-1}A = \nu + \theta + \gamma \tag{16}$$

$$\cos^{-1}C = \nu + \theta - \gamma \tag{17}$$

$$\cos^{-1}F = \nu - \theta + \gamma \tag{18}$$

$$\cos^{-1}E = \nu - \theta - \gamma \tag{19}$$

and

$$\theta = \frac{\cos^{-1}A - \cos^{-1}F}{2} \tag{20}$$

$$\nu = \frac{\cos^{-1}A + \cos^{-1}E}{2} \tag{21a}$$

$$\nu = \frac{\cos^{-1}C + \cos^{-1}F}{2} \tag{21b}$$

In order to insure greater accuracy care should be taken to avoid the portions of the curve where $\cos \epsilon(t) \approx 1$. For instance, for figure 4 equations (20) and (21b) should be used.

Case II. $\nu < \theta + \gamma$ where $\gamma > \theta$

The equations become

$$\cos^{-1}A = \nu + \theta + \gamma \tag{22}$$

$$\cos^{-1}C = \pm(\nu + \theta - \gamma) \tag{23}$$

$$\cos^{-1}F = \nu - \theta + \gamma \tag{24}$$

$$\cos^{-1}E = -(\nu - \theta - \gamma) \tag{25}$$

and

$$\theta = \frac{\cos^{-1}A - \cos^{-1}F}{2} \tag{26}$$

$$\nu = \frac{\cos^{-1}A - \cos^{-1}E}{2} \tag{27}$$

Equation (23) may be used together with equations (22) and (27) to determine θ to a greater degree of accuracy as long as equation (26) is used to determine the correct sign to be used in equation (23).

Case III. $\nu < \theta + \gamma$ where $\theta > \gamma$

Equations (12) to (15) become

$$\cos^{-1}A = \nu + \theta + \gamma \tag{28}$$

$$\cos^{-1}C = \nu + \theta - \gamma \tag{29}$$

$$\cos^{-1}F = \pm(\nu - \theta + \gamma) \tag{30}$$

$$\cos^{-1}E = -(\nu - \theta - \gamma) \tag{31}$$

and

$$\nu = \frac{\cos^{-1}A - \cos^{-1}E}{2} \tag{32}$$

$$\theta = \frac{\cos^{-1}A + \cos^{-1}C}{2} - \nu \tag{33a}$$

or

$$\theta = \frac{\cos^{-1}A + \cos^{-1}E}{2} - \gamma \tag{33b}$$

In each one of the cases the additional equations can be used as a cross-check of the solution and to insure greater accuracy.

The choice of which case will apply will depend on the trajectory. For instance, in the case of a due east launch, ν turns out to be approximately 90° and for $\gamma = \tan^{-1}\sqrt{2}$, equations (16) to (19) would apply for small values of θ.

Special Case

Further simplification of cases I and III can be obtained by letting $\gamma = 0$ (probe mounted parallel to the spin axis of the body).

With $\gamma = 0$ and $B = 1$ equations (2) and (5) become

$$B_p = \cos \nu \cos \theta - \sin \nu \sin \theta \cos \psi \tag{34}$$

Here B_p is a function of only ν, θ, and ψ. A typical curve for $\gamma = 0$ is shown in figure 6. There are two points of interest on this curve. These occur when $\psi = 0$ and when $\psi = \pi$. The equations become

$$B_{p,1} = \cos \nu \cos \theta + \sin \nu \sin \theta \qquad \psi = \pi \tag{35}$$

and

$$B_{p,2} = \cos \nu \cos \theta - \sin \nu \sin \theta \qquad \psi = 0 \qquad (36)$$

These can be reduced to

$$B_{p,1} = \cos(\nu - \theta) \qquad (37)$$

$$B_{p,2} = \cos(\nu + \theta) \qquad (38)$$

respectively.

Equations (37) and (38) may be solved simultaneously to yield for $\nu > \theta$

$$\theta = \frac{\cos^{-1}B_{p,2} - \cos^{-1}B_{p,1}}{2} \qquad (39)$$

$$\nu = \cos^{-1}B_{p,1} + \theta \qquad (40)$$

and for $\nu < \theta$

$$\theta = \frac{\cos^{-1}B_{p,2} + \cos^{-1}B_{p,1}}{2} \qquad (41)$$

$$\nu = \frac{\cos^{-1}B_{p,2} - \cos^{-1}B_{p,1}}{2} \qquad (42)$$

From the viewpoint of the present analysis the probe should be placed at $\gamma = 0$ only in the case where the value of B is known to a reasonable degree of accuracy. In this case, which occurs frequently, putting $\gamma = 0$ offers a distinct advantage over placing the probe at any other angle. The resulting curve is greatly simplified and therefore requires less interpretation. However, in this case, the spin rate cannot be determined directly from the magnetometer trace but must be either found by some other method, or inferred from equation (1).

LIMITATIONS OF THE METHOD

There are some possible sources of error associated with this method which could limit its range of application. The chief sources of error are:

(a) Fairing error. The method should be applied only when $p_0 \gg \omega_p$. For instance, $p_0 = 4\omega_p$ would give five fairing points for each precession cycle and would seem to be a minimum condition for application of the method. This limitation is not too severe since many vehicles now being flown are within this condition.

(b) Error in magnitude of $\overline{B}$. Because an arc cosine is inherently inaccurate for small angles, an error due to uncertainty in the magnitude of the field can be magnified; therefore, values of $\epsilon(t)$ near zero should be avoided.

(c) Instrument error. It is reported in reference 7 that the magnetometer-instrument error should be less than $\pm 1^{\circ}$.

The effects of these errors on the uncertainty in the values of θ and ν can be evaluated in the same manner for each of three types of errors. The calculation of the effect of instrument error will be presented here as a sample.

The instrument error of $\pm 1^{\circ}$ will be considered to be a three standard deviation in ϵ (i.e., $3\sigma_{\epsilon} = \pm 1^{\circ}$). The effect of this error can be evaluated from equations (16) to (33b). For case I, a change in θ of $\Delta\theta$ due to changes ΔA and ΔF can be calculated from equation (20) to be

$$\Delta\theta = \frac{1}{2}\left(\frac{\Delta F}{\sqrt{1 - F^2}} - \frac{\Delta A}{\sqrt{1 - A^2}}\right) \tag{43}$$

The value of ΔA and ΔF can be found from equations (8) and (10), respectively, to be,

$$\Delta A = -\sqrt{1 - A^2}\,\Delta\epsilon_A \tag{44}$$

$$\Delta F = -\sqrt{1 - F^2}\,\Delta\epsilon_F \tag{45}$$

Substitution for ΔA and ΔF yields

$$\Delta\theta = \frac{1}{2}\left(-\Delta\epsilon_A + \Delta\epsilon_F\right) \tag{46}$$

This equation would yield the change in θ due to a known change in $\epsilon(t)$ at the points A and F. In practice, however, only the standard deviation of ϵ will be known. Therefore (ref. 8)

$$\sigma_\theta^2 = \left(\frac{\partial\theta}{\partial A}\right)^2 \sigma_A^2 + \left(\frac{\partial\theta}{\partial F}\right)^2 \sigma_F^2$$

$$= \left(\frac{\partial\theta}{\partial\epsilon_A}\right)^2 \sigma_{\epsilon,A}^2 + \left(\frac{\partial\theta}{\partial\epsilon_F}\right)^2 \sigma_{\epsilon,F}^2 \tag{47}$$

and from equation (46)

$$\frac{\partial\theta}{\partial\epsilon_A} = -\frac{1}{2}, \quad \frac{\partial\theta}{\partial\epsilon_F} = \frac{1}{2}$$

hence

$$\sigma_\theta^2 = \frac{\sigma_{\epsilon,A}^2}{4} + \frac{\sigma_{\epsilon,F}^2}{4} = \frac{\sigma_\epsilon^2}{2}$$

or

$$\sigma_\theta = \frac{\sigma_\epsilon}{\sqrt{2}} \tag{48}$$

If this procedure is used to find σ_θ and σ_ν for cases I, II, and III, the results are,

For case I:

$$\sigma_\theta = \frac{\sigma_\epsilon}{\sqrt{2}} \qquad \text{from equation (20)}$$

$$\sigma_\nu = \frac{\sigma_\epsilon}{\sqrt{2}} \qquad \text{from equations (21a) or (21b)}$$

For case II:

$$\sigma_\theta = \frac{\sigma_\epsilon}{\sqrt{2}} \qquad \text{from equation (26)}$$

$$\sigma_\nu = \frac{\sigma_\epsilon}{\sqrt{2}} \qquad \text{from equation (27)}$$

For case III:

$$\sigma_\nu = \frac{\sigma_\epsilon}{\sqrt{2}} \qquad \text{from equation (32)}$$

$$\sigma_\theta = \sqrt{2}\,\sigma_\epsilon \qquad \text{from equation (33a)}$$

$$\sigma_\theta = \frac{\sigma_\epsilon}{\sqrt{2}} \qquad \text{from equation (33b)}$$

with the assumption $3\sigma_\epsilon = \pm 1^\circ$, or $\sigma_\epsilon = \pm\frac{1^\circ}{3}$, it can easily be seen that

$$\sigma_\theta = \pm 0.235^\circ \text{ or } \pm 0.47^\circ$$

$$\sigma_\nu = \pm 0.235^\circ$$

CONCLUDING REMARKS

The use of an onboard magnetometer has been considered for determining the motion of spinning bodies in uniform precession. Typical types of magnetometer output histories are presented for magnetometers mounted at a known angle to the spin axis. These curves were analyzed and a general method was developed for determining both the body coning angle and the angle between the local magnetic vector and the body angular momentum vector.

In the case where B, the magnitude of the local magnetic vector, is known, the body coning angle θ and the angle between the earth's local magnetic vector and the angular-momentum vector of the body ν can be determined from the envelope of the magnetometer signal.

A greatly simplified curve can be obtained if the angle between the magnetometer probe direction and the longitudinal axis of the body is zero. This case can also be analyzed to give ν and θ.

For an accurate analysis, magnetometer readings very close to $\pm B$ (corresponding to an angle between the magnetometer probe axis and the local magnetic field near 0° or 180°) should be avoided, since these angles cannot be accurately determined from their cosines.

Langley Research Center,
National Aeronautics and Space Administration,
Langley Station, Hampton, Va., February 7, 1964.

REFERENCES

1. Israel, G., and Vassy, A.: Résultats concernant l'attitude d'une Fusée Véronique obtenus au moyen de capteurs magnétiques. Astronautica Acta, vol. 8, no. 5, 1962, pp. 264-277.

2. Beletskii, V. V., and Zonov, Yu. V.: Rotation and Orientation of the Third Soviet Satellite. Lib. Translation No. 984, British R.A.E., Jan. 1962.

3. Heppner, J. P., Skillman, T. L., and Cain, J. C.: Contributions of Rockets and Satellites to the World Magnetic Survey. NASA TN D-705, 1961.

4. White, John S., Shigemoto, Fred H., and Bourquin, Kent: Satellite Attitude Control Utilizing the Earth's Magnetic Field. NASA TN D-1068, 1961.

5. Ito, M.: Analysis of the Output of Rocket-Borne Magnetometers. Canadian Jour. of Phys., vol. 41, no. 8, Aug. 1963, pp. 1252-1262.

6. Buglia, James J., Young, George R., Timmons, Jesse D., and Brinkworth, Helen S.: Analytical Method of Approximating the Motion of a Spinning Vehicle With Variable Mass and Inertia Properties Acted Upon by Several Disturbing Parameters. NASA TR R-110, 1961.

7. Asquith, C. F., and Baxter, W. F.: Missile Attitude Determination Using Magnetometers With Sun and Earth Sensors. RG-TR-62-5, U.S. Army Missile Command (Redstone Arsenal, Ala.), Dec. 31, 1962.

8. Hald, A.: Statistical Theory With Engineering Applications. John Wiley & Sons, Inc., c.1952.

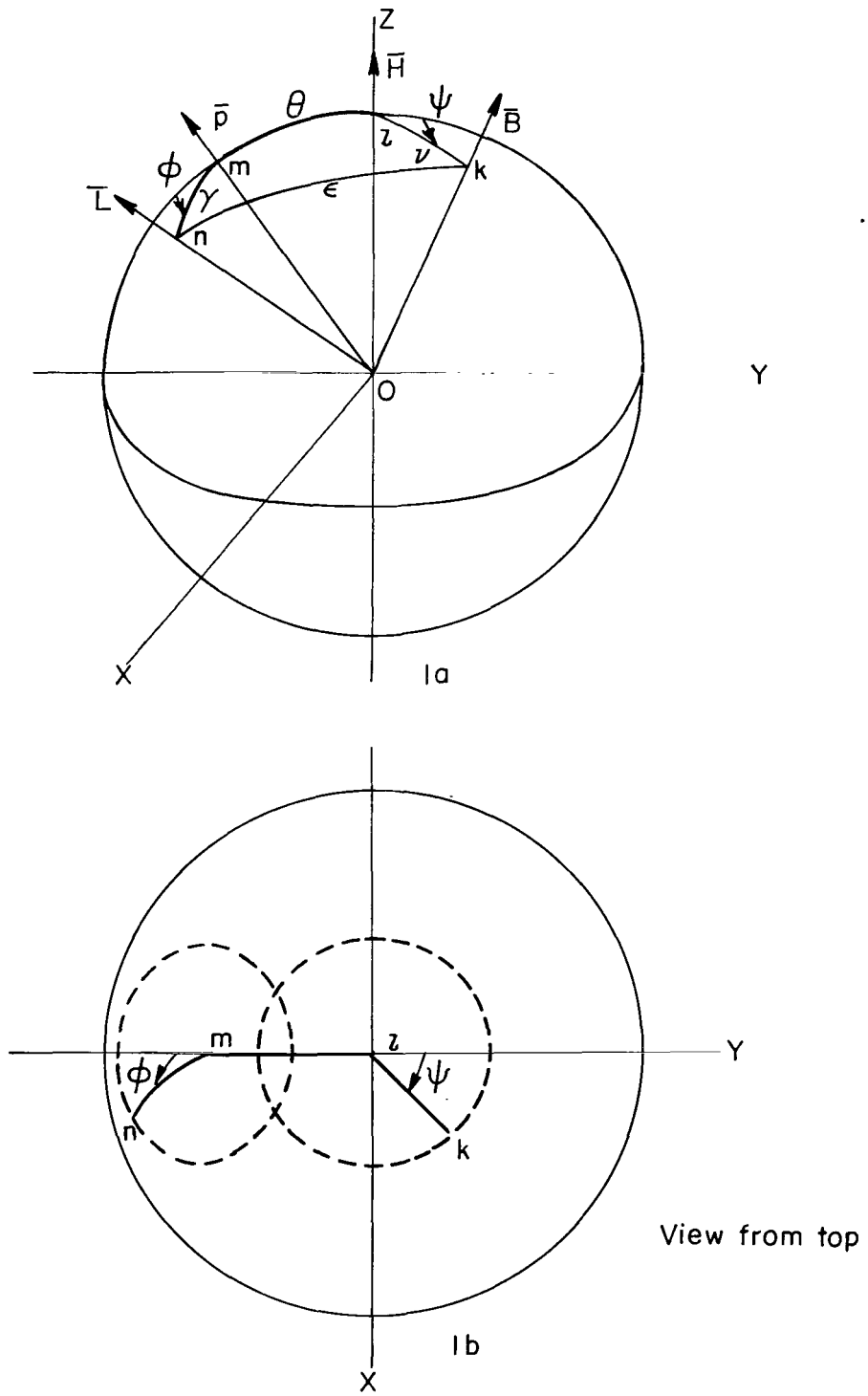

Figure 1.- Angles used in analysis projected onto a unit sphere.

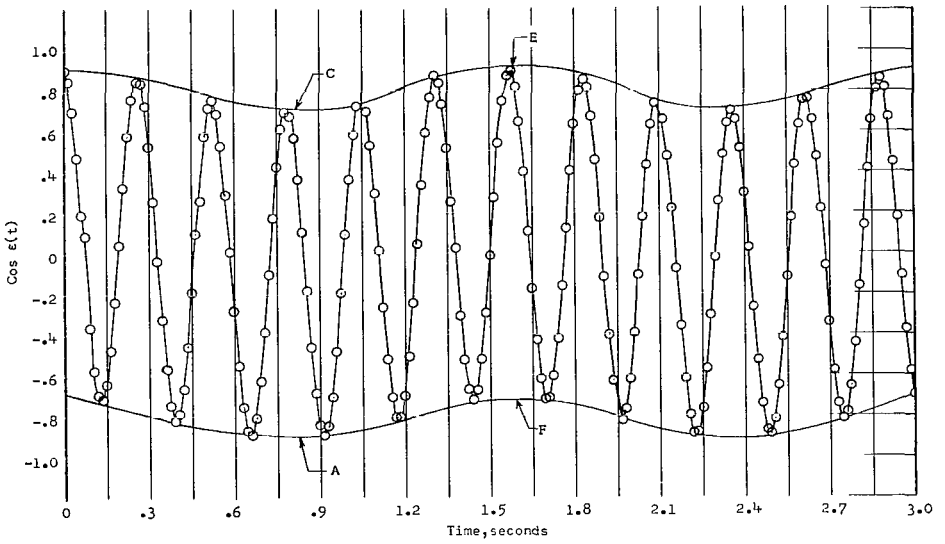

(a) Magnetometer signal as a function of time.

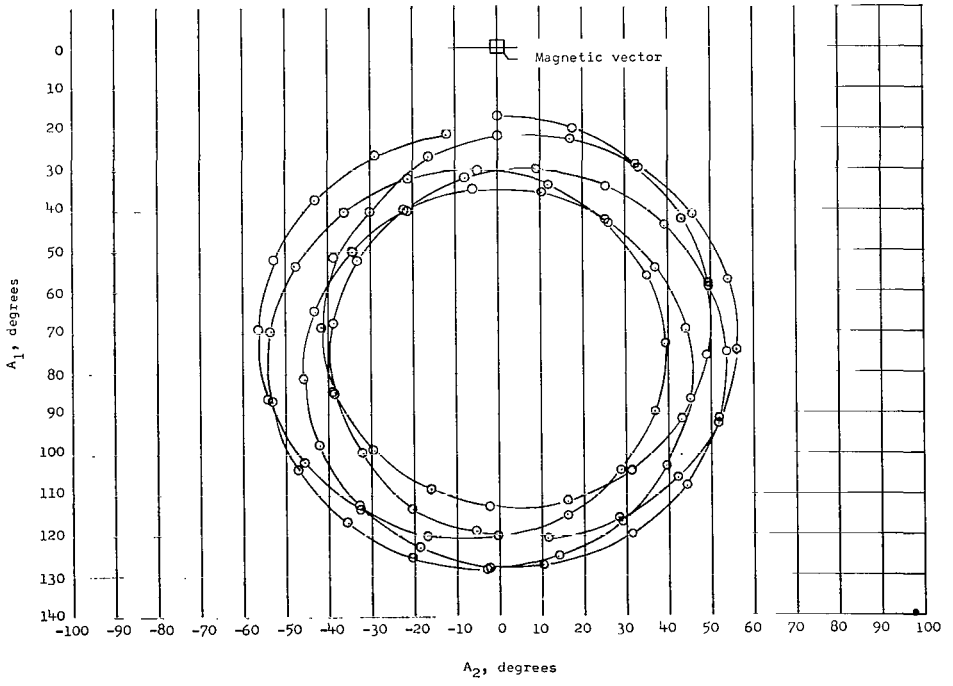

(b) Schematic of approximate motion of tip of probe vector in space.

Figure 2.- Magnetometer signal and schematic of approximate probe motion for $\nu = 90^\circ$, $\theta = 10^\circ$, and $\gamma = 54.8^\circ$.

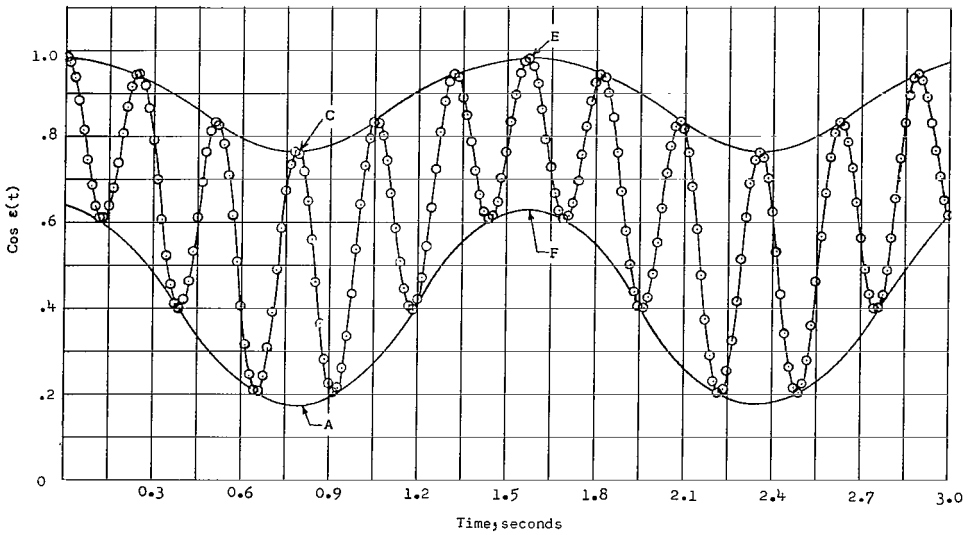

(a) Magnetometer signal as a function of time.

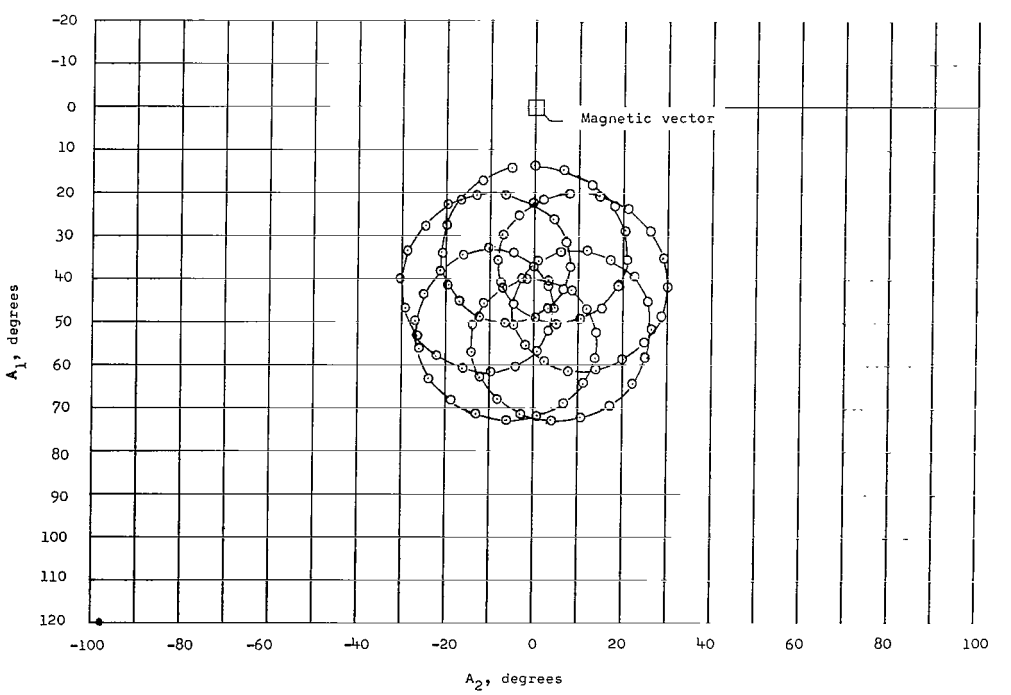

(b) Schematic of approximate motion of tip of probe vector in space.

Figure 3.- Magnetometer signal and schematic of approximate probe motion for $\nu = 45^\circ$, $\theta = 15^\circ$, and $\gamma = 20^\circ$.

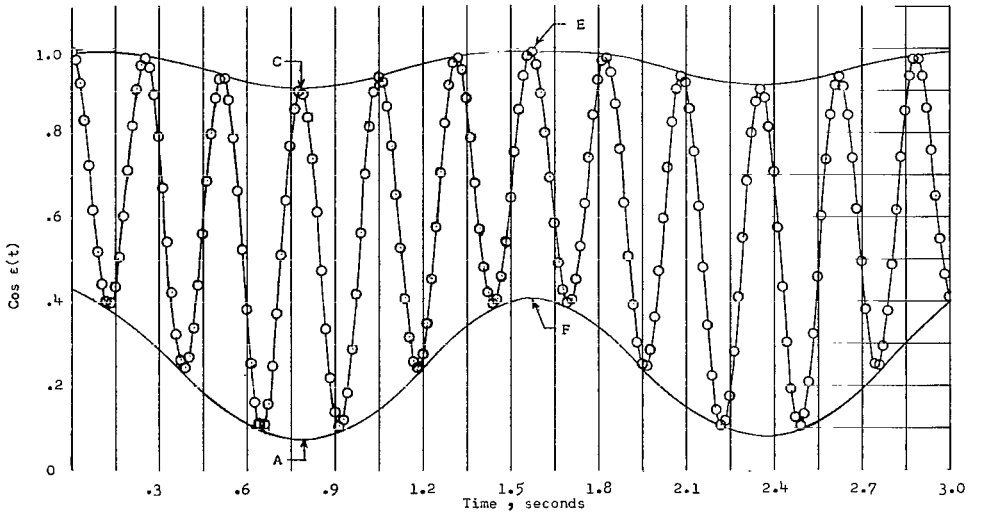

(a) Magnetometer signal as a function of time.

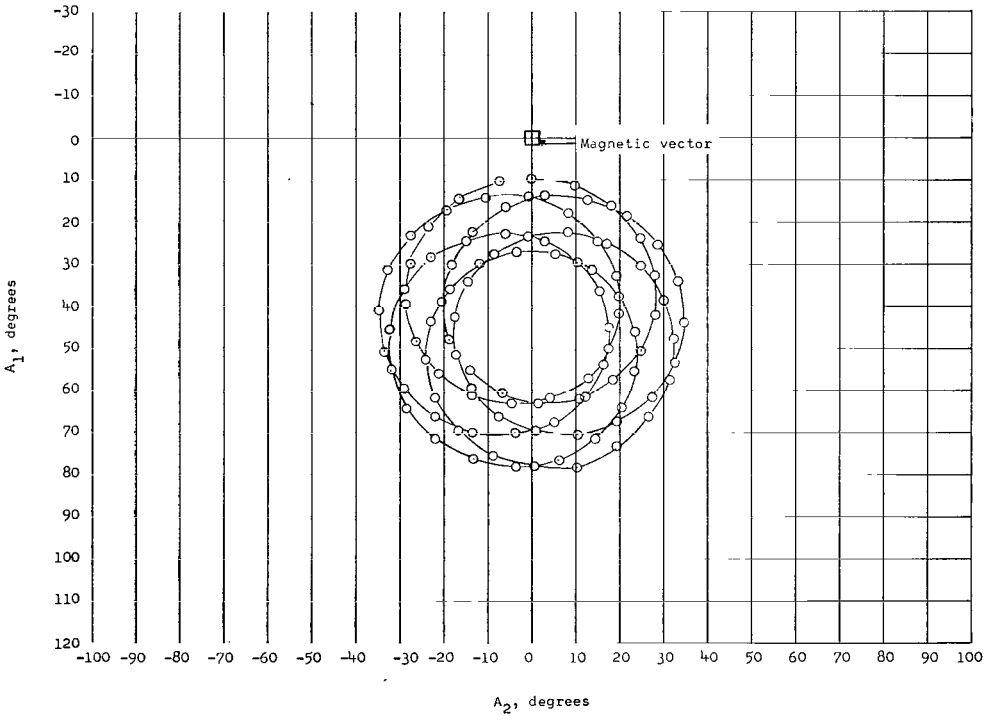

(b) Schematic of approximate motion of tip of probe vector in space.

Figure 4.- Magnetometer signal and schematic of approximate probe motion for $\nu = 45^{\circ}$, $\theta = 10^{\circ}$, and $\gamma = 30^{\circ}$.

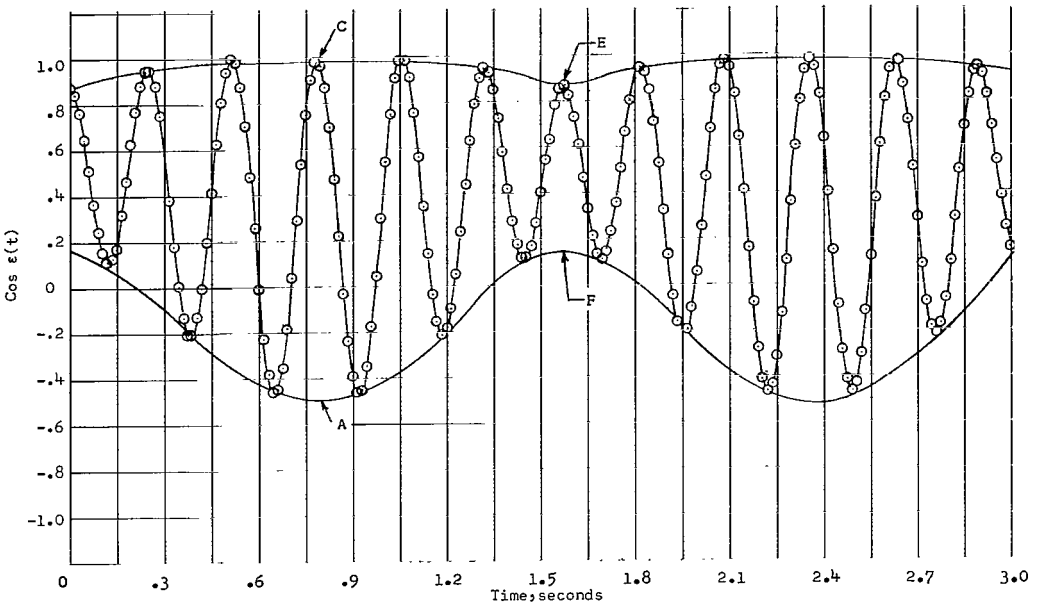

(a) Magnetometer signal as a function of time.

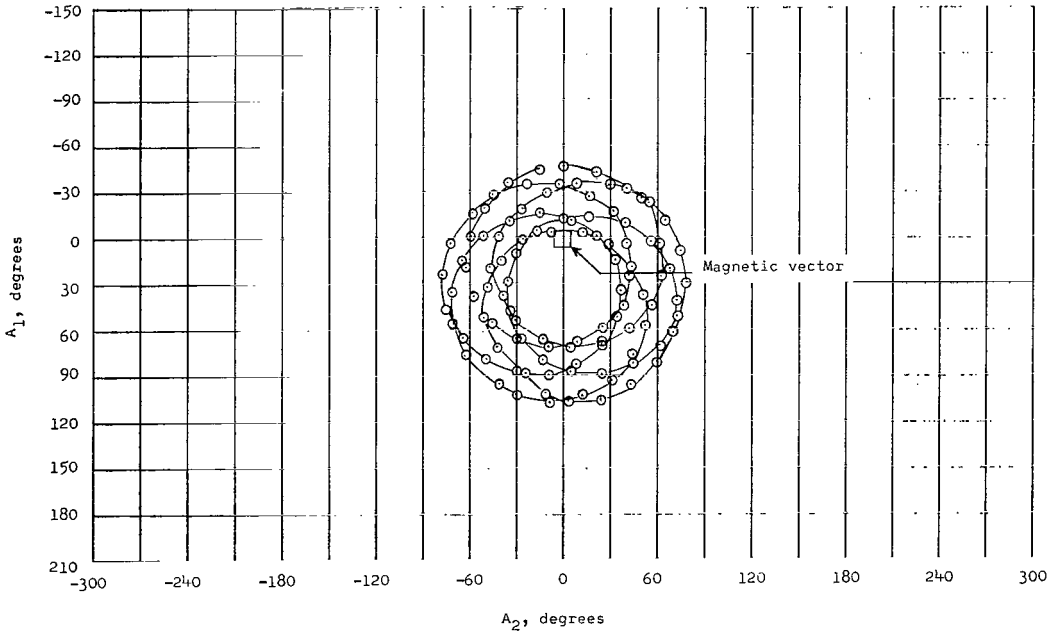

(b) Schematic of approximate motion of tip of probe vector in space.

Figure 5.- Magnetometer signal and schematic of approximate probe motion for $\nu = 45^\circ$, $\theta = 20^\circ$, and $\gamma = 54.8^\circ$.

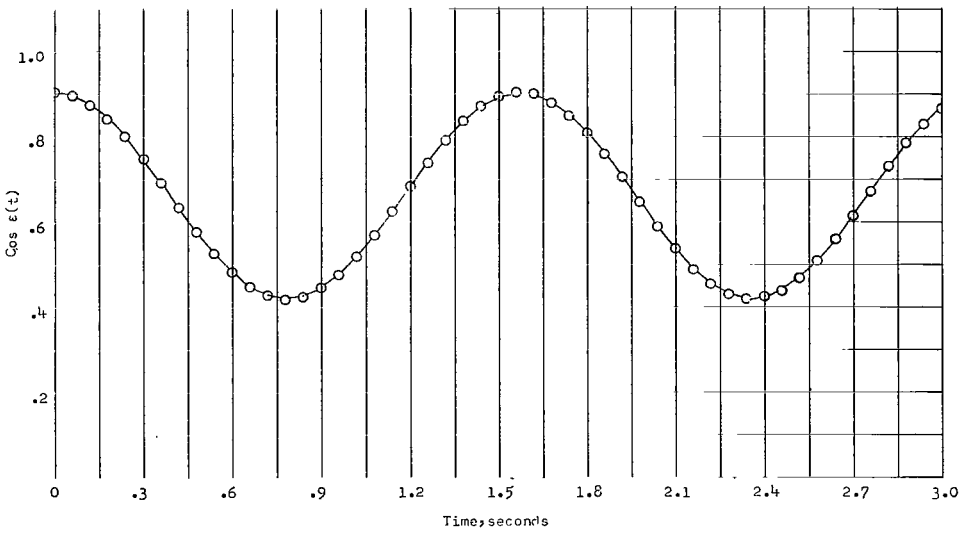

(a) Magnetometer signal as a function of time.

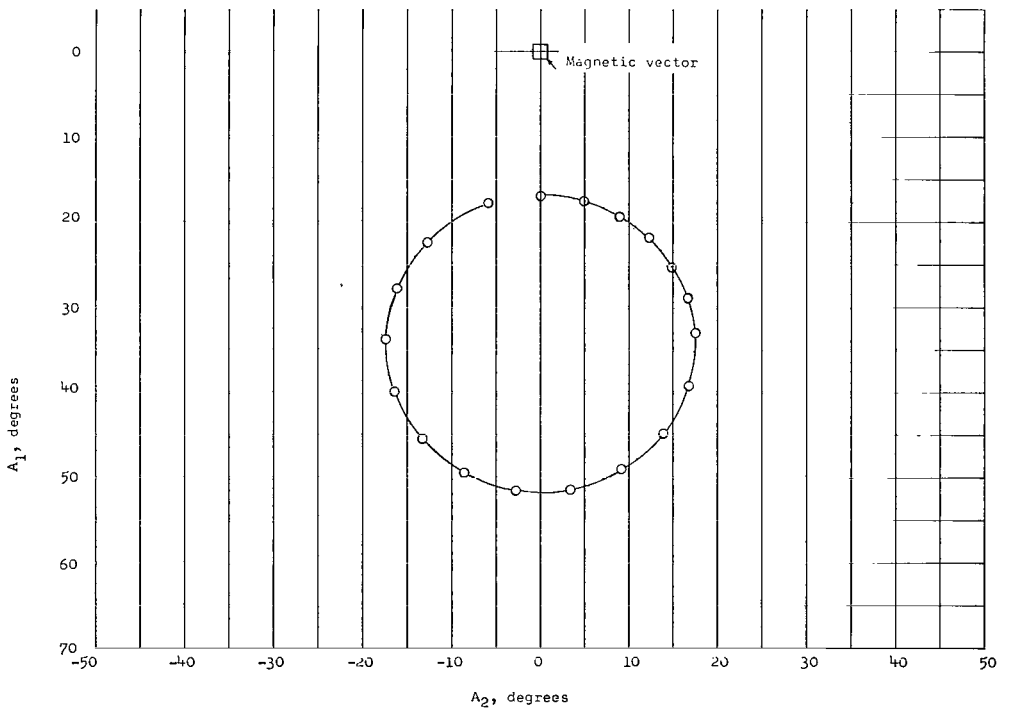

(b) Schematic of approximate motion of tip of probe vector in space.

Figure 6.- Magnetometer signal and schematic of approximate probe motion for $\nu = 45^\circ$, $\theta = 20^\circ$, and $\gamma = 0^\circ$.

"The National Aeronautics and Space Administration . . . shall . . . provide for the widest practical appropriate dissemination of information concerning its activities and the results thereof . . . objectives being the expansion of human knowledge of phenomena in the atmosphere and space."

—National Aeronautics and Space Act of 1958

NASA SCIENTIFIC AND TECHNICAL PUBLICATIONS

TECHNICAL REPORTS: Scientific and technical information considered important, complete, and a lasting contribution to existing knowledge.

TECHNICAL NOTES: Information less broad in scope but nevertheless of importance as a contribution to existing knowledge.

TECHNICAL MEMORANDUMS: Information receiving limited distribution because of preliminary data, security classification, or other reasons.

CONTRACTOR REPORTS: Technical information generated in connection with a NASA contract or grant and released under NASA auspices.

TECHNICAL TRANSLATIONS: Information published in a foreign language considered to merit NASA distribution in English.

TECHNICAL REPRINTS: Information derived from NASA activities and initially published in the form of journal articles or meeting papers.

SPECIAL PUBLICATIONS: Information derived from or of value to NASA activities but not necessarily reporting the results of individual NASA-programmed scientific efforts. Publications include conference proceedings, monographs, data compilations, handbooks, sourcebooks, and special bibliographies.

Details on the availability of these publications may be obtained from:

SCIENTIFIC AND TECHNICAL INFORMATION DIVISION

NATIONAL AERONAUTICS AND SPACE ADMINISTRATION

Washington, D.C. 20546